Pool film boiling from spheres to saturated and subcooled liquids of Freon-12 and Freon-22

C. P. Tso, H. G. Low, and S. M. Ng
Department of Mechanical Engineering, University of Malaya, Kuala Lumpur, Malaysia

A combined analytical and experimental study of pool film boiling from spheres is reported. Analytical solutions for subcooled and saturated boiling are obtained by applying an integral method to the two-phase boundary layer around a sphere. Results are compared to experimental data obtained in the authors' laboratory for atmospheric boiling in Freon-12 and Freon-22, as well as to published data on water, Freon-11, and liquid nitrogen.

Keywords: film boiling; boiling over spheres; boiling in Freon-12 and Freon-22; two-phase layer flow

Introduction

Film boiling heat transfer has been studied extensively, but the theory is still disputed. Since Bromley,[1] the early theoretical work reported was based on applying the boundary layer equations to the two-phase boundary layer along a vertical surface[2,3] and along a horizontal cylinder,[4] where the equations were finally solved numerically.

However, an analytical solution was obtained for the case of natural convection, saturated film boiling on a sphere[5] by simplification of the boundary layer equations and balancing of integral momentum and energy. Later, this type of analysis was extended to cases involving both linear and quadratic velocity and temperature profiles across the vapor film around the sphere.[6] Four cases were analyzed and the results compared to experimental data. We use a similar analysis here. More recently, a numerical solution of an integral method was applied to the sphere, among other curved surfaces.[7]

Analytical solutions for film boiling in subcooled liquids based on the integral method in a vertical plane only had been reported in the Japanese literature.[8] In this analysis we present the detailed solution to the sphere case, although the results alone had been mentioned earlier.[9] Faced with an abundance of reported experimental work,[10] our comparison of the foregoing solutions will use selected data on Freon-11,[11] nitrogen,[6] and water,[9] and our recent data on Freon-12 and Freon-22, obtained by the quenching method under normal atmospheric conditions.

Theoretical analysis

Figure 1 shows the physical model and coordinates, with the sphere radius, vapor layer thickness and liquid layer thickness being R, Δ, and δ, respectively. Based on the assumptions of thin layers in an incompressible fluid and no radiation effects, the one-dimensional (1-D) laminar momentum and energy boundary layer equations for the buoyancy-induced vapor motion are

$$\rho_v u_v \frac{\partial u_v}{\partial x} = g(\rho_l - \rho_v) \sin \phi + \mu_v \frac{\partial^2 u_v}{\partial y^2} \tag{1}$$

Address reprint requests to Dr. Tso at the Department of Mechanical Engineering, University of Malaya, 59100 Kuala Lumpur, Malaysia.

Received 29 August 1989; accepted 20 December 1989

$$\rho_v c_{pv} u_v \frac{\partial T_v}{\partial x} = k_v \frac{\partial^2 T_v}{\partial y^2} \tag{2}$$

The corresponding equations for the free-convection equations for the liquid layer are

$$\rho_l u_l \frac{\partial u_l}{\partial x} = g\beta_l \rho_l (T_l - T_\infty) \sin \phi + \mu_l \frac{\partial^2 u_l}{\partial z^2} \tag{3}$$

$$\rho_l c_{pl} u_l \frac{\partial T_l}{\partial x} = k_l \frac{\partial^2 T_l}{\partial z^2} \tag{4}$$

To effect an analytical solution, we make the following further assumptions.

(1) Convective terms (on the left side) are neglected, and the effects are compensated for by using an effective latent heat of vaporization,[5] or

$$h_{fg}^* = h_{fg} + 0.5 c_{pv} \Delta T_{sat} \tag{5}$$

in a later energy balancing (Equation 17).

(2) The Boussinesq term in the liquid momentum equation is neglected, thereby decoupling the equations for the liquid layer.

(3) The wall temperature is uniform at T_w, and the vapor–liquid interface is smooth and is at T_{sat} ($T_w > T_{sat} > T_\infty$).

(4) The thickness of the velocity boundary layer is assumed to be the same as that of the thermal boundary layer.

The necessary velocity boundary conditions are assumed to be the no-slip condition at the wall and at the vapor–liquid interface, continuous interfacial shear, and stationary bulk liquid beyond the boundary of the liquid layer. The full set of conditions follows.

At $y = 0$: $u_v = 0$ (6)

$$T_v = T_w \tag{7}$$

At $y = \Delta$: $u_v = u_l$ (8)

$$\mu_v \frac{\partial u_v}{\partial y} = \mu_l \frac{\partial u_l}{\partial z} \tag{9}$$

$$T_v = T_l = T_{sat} \tag{10}$$

At $z = \delta$: $u_l = 0$ (11)

$$T_l = T_\infty \tag{12}$$

The governing equations may now be solved completely in

terms of the unknowns Δ and δ. The results are

$$u_v = \frac{g(\rho_l - \rho_v)\sin\phi\Delta^2}{2\mu_v}\left[\left(\frac{f+2\xi}{f+\xi}\right)\left(\frac{y}{\Delta}\right) - \left(\frac{y}{\Delta}\right)^2\right] \tag{13}$$

$$T_v = T_w - \Delta T_{sat}\frac{y}{\Delta} \tag{14}$$

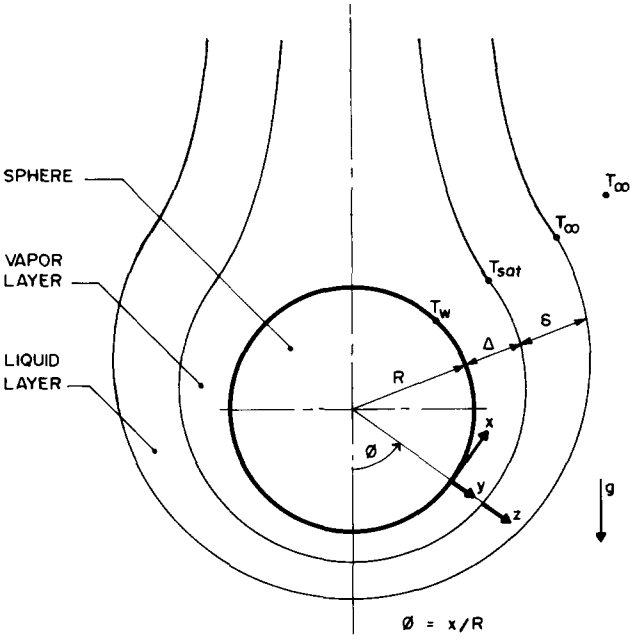

Figure 1 Physical model and coordinate system for subcooled film boiling

$$u_l = \frac{g(\rho_l - \rho_v)\sin\phi\Delta^2}{2\mu_l}\left(\frac{f\xi}{f+\xi}\right)\left(1 - \frac{z}{\delta}\right) \tag{15}$$

$$T_l = T_{sat} - \Delta T_{sub}\frac{z}{\delta} \tag{16}$$

where $f = \mu_l/\mu_v$ and $\xi = \delta/\Delta$. The model implies linear temperature and liquid velocity profiles but a quadratic vapor velocity profile.

Next, integral heat balances are performed on the vapor and liquid layers, giving

$$h^*_{fg}\frac{d}{dx}\int_0^\Delta u_v\rho_v 2\pi R\sin\phi\, dy = 2\pi R\sin\phi\left[-k_v\left.\frac{\partial T_v}{\partial y}\right|_{y=0} + k_l\left.\frac{\partial T_l}{\partial z}\right|_{z=0}\right] \tag{17}$$

$$c_{p_l}\frac{d}{dx}\int_0^\delta u_l\rho_l(T_l - T_\infty)2\pi R\sin\phi\, dz = 2\pi R\sin\phi\left[-k_l\left.\frac{\partial T_l}{\partial z}\right|_{z=0}\right] \tag{18}$$

Substituting Equations 13–16 into Equations 17 and 18, and assuming ξ to be independent of x, yields

$$\frac{d}{dx}\Delta^3\sin^2\phi = \left(\frac{f+\xi}{f+4\xi}\right)\left[\frac{12\mu_v k_v\Delta T_{sat}}{g(\rho_l-\rho_v)h^*_{fg}\rho_v} - \frac{12\mu_v k_l\Delta T_{sub}}{g(\rho_l-\rho_v)h^*_{fg}\rho_v\xi}\right]\frac{\sin\phi}{\Delta} \tag{19}$$

$$\frac{d}{dx}\Delta^3\sin^2\phi = \left(\frac{f+\xi}{f\xi^2}\right)\left(\frac{6\mu_l k_l}{c_{p_l}\rho_l g(\rho_v-\rho_l)\xi}\right)\frac{\sin\phi}{\Delta} \tag{20}$$

The solutions to Equations 19 and 20, respectively, are

$$\Delta = I(\phi)\left\{\frac{f+\xi}{f+4\xi}\left[\frac{16\mu_v k_v R\,\Delta T_{sat}}{g(\rho_l-\rho_v)h^*_{fg}\rho_v} - \frac{16\mu_v k_l R\,\Delta T_{sub}}{g(\rho_l-\rho_v)h^*_{fg}\rho_v\xi}\right]\right\}^{1/4} \tag{21}$$

Notation

b	Parameter defined by Equation 40
c	Numerical constant in Equation 46
c_p	Specific heat at constant pressure
C_1	Parameter defined by Equation 27
C_2	Parameter defined by Equation 28
C_3	Parameter defined by Equation 29
C_o	Coefficient in Equation 33, defined by Equation 41
C'_o	Coefficient in Equation 47
D	Diameter of sphere
f	Ratio of viscosity, μ_l/μ_v
F_1	Parameter defined by Equation 38
F_2	Parameter defined by Equation 39
g	Acceleration due to gravity
Gr_D	Grashof number, $g(\rho_l-\rho_v)\rho_v D^3/\mu_v^2$
h	Convective heat transfer coefficient
h_{fg}	Latent heat of vaporization
h^*_{fg}	Modified latent heat of vaporization, defined by Equation 5
$I(\phi)$	Parameter defined by Equation 23
J	Dimensionless parameter defined by Equation 34
k	Thermal conductivity
m	Dimensionless parameter defined by Equation 36
Nu_D	Nusselt number, hD/k
Pr	Prandtl number
Pr*	Modified Prandtl number, defined by Equation 48
q''_x	Local heat flux
R	Radius of sphere
S_c	Dimensionless parameter defined by Equation 37
S_p	Dimensionless parameter defined by Equation 35
T	Temperature
T_{sat}	Saturation temperature
T_w	Wall temperature
T_∞	Ambient liquid temperature
ΔT_{sat}	Degree above saturation, $T_w - T_{sat}$
ΔT_{sub}	Degree of subcooling, $T_{sat} - T_\infty$
u	Velocity
W_1	Parameter defined by Equation 25
W_2	Parameter defined by Equation 26
x	Circumferential direction, as in Figure 1
y	Radial direction, as in Figure 1
z	Radial direction, as in Figure 1

Greek symbols

β	Volume coefficient of expansion
δ	Thickness of liquid film
Δ	Thickness of vapor film
μ	Dynamic viscosity
ξ	Ratio of thicknesses, δ/Δ
ρ	Density
ϕ	Azimuthal angle from sphere bottom

Subscripts

l	Referring to liquid
v	Referring to vapor

Overbar denotes average quantity.

$$\Delta = I(\phi)\left\{\frac{f+\xi}{f\xi^2}\left[\frac{8\mu_l k_l R}{c_{p_l}\rho_l g(\rho_v-\rho_l)\xi}\right]\right\}^{1/4} \tag{22}$$

where

$$I(\phi)=\frac{(\int \sin^{5/3}\phi\, d\phi)^{1/4}}{\sin^{2/3}\phi} \tag{23}$$

Equating Equations 21 and 22 produces a cubic equation in ξ, which has at least one real root:

$$\xi=(W_1+W_2^{1/2})^{1/3}+(W_1-W_2^{1/2})^{1/3}+\frac{k_l\,\Delta T_{\text{sub}}}{3k_v\,\Delta T_{\text{sat}}} \tag{24}$$

where

$$W_1=\left(\frac{C_2}{3C_1}\right)^3+\frac{2C_2C_3}{3C_1^2 f}+\frac{C_3}{2C_1} \tag{25}$$

$$W_2=\left(\frac{C_3}{2C_1}\right)^2+\left(\frac{C_3}{C_1}\right)\left(\frac{C_2}{3C_1}\right)^3 +\left(\frac{C_3^2}{fC_1^3}\right)\left[\frac{2C_2}{3}-\frac{4C_2^2}{27fC_1}-\frac{64C_3}{27f^2}\right] \tag{26}$$

$$C_1=\frac{12\mu_v k_v\,\Delta T_{\text{sat}}}{g(\rho_l-\rho_v)h_{fg}^*\rho_v} \tag{27}$$

$$C_2=\frac{12\mu_v k_l\,\Delta T_{\text{sub}}}{g(\rho_l-\rho_v)h_{fg}^*\rho_v} \tag{28}$$

$$C_3=\frac{6\mu_l k_l}{g(\rho_l-\rho_v)c_{p_l}\rho_l} \tag{29}$$

Turning now to evaluation of the heat transfer coefficient, we see that the average heat flux from the sphere surface is

$$\bar{q}_x''=\frac{1}{(4\pi R^2)}\int_0^\pi (2\pi R\sin\phi)R\,d\phi\left(-k_v\left.\frac{\partial T_v}{\partial y}\right|_{y=0}\right) =\tfrac{1}{2}k_v\,\Delta T_{\text{sat}}\int_0^\pi \frac{\sin\phi}{\Delta}\,d\phi \tag{30}$$

Hence the average Nusselt number is

$$\overline{\text{Nu}_D}=\frac{\bar{h}D}{k_v}=\left(\frac{\bar{q}_x''}{\Delta T_{\text{sat}}}\right)\frac{D}{k_v} =\tfrac{1}{2}D\int_0^\pi \frac{\sin\phi}{\Delta}\,d\phi \tag{31}$$

Substituting Equation 22 into Equation 31 yields

$$\overline{\text{Nu}_D}=\tfrac{1}{2}D(\text{Gr}_D\text{Pr}_v)^{1/4}\left[(4D^4)\left(\frac{f+\xi}{\xi^3}\right)\left(\frac{k_l c_{p_v}\rho_v)}{k_v c_{p_l}\rho_l}\right)\right]^{-1/4}\int_0^\pi \frac{\sin\phi}{I(\phi)}\,d\phi \tag{32}$$

By using Equation 24 and rearranging Equation 32, we can write Equation 32 in final form as

$$\frac{\overline{\text{Nu}_D}}{(\text{Gr}_D\text{Pr}_v)^{1/4}}=C_o\left[\frac{J^3}{m^2\text{Pr}_l^2\text{Pr}_v S_p^3(1+J/S_p\text{Pr}_l)}\right]^{1/4} \tag{33}$$

where

$$J=(F_1+bF_2^{1/2})^{1/3}+(F_1-bF_2^{1/2})^{1/3}+\frac{S_c}{3} \tag{34}$$

$$S_p=\frac{c_{p_v}\,\Delta T_{\text{sat}}}{h_{fg}^*\text{Pr}_v} \tag{35}$$

$$m=\left(\frac{\rho_v\mu_v}{\rho_l\mu_l}\right)^{1/2} \tag{36}$$

$$S_c=\frac{c_{p_l}\,\Delta T_{\text{sub}}}{h_{fg}^*} \tag{37}$$

$$F_1=\frac{S_p^3\text{Pr}_l^3 W_1}{f^3} \tag{38}$$

$$F_2=\frac{64S_p^4\text{Pr}_l^4 W_2}{m^4 f^6} \tag{39}$$

$$b=\frac{m^2 S_p\text{Pr}_l}{8} \tag{40}$$

$$C_o=2^{-3/2}\int_0^\pi \frac{\sin\phi}{I(\phi)}\,d\phi=0.696 \tag{41}$$

Special case of saturated boiling

The case of saturated film boiling may be regarded as a special case of subcooled film boiling, simply by considering only a vapor layer around the sphere, as shown in Figure 2. As the theory for this case is available in the literature,[5,6] we will present only a brief outline here. Equations 1, 2, and 17 are applied to the vapor layer, except that in Equation 17 the last term, $k_l\,\partial T_l/\partial z$, vanishes. The assumption is that heat is not conducted to the saturated liquid beyond the vapor–liquid interface. The boundary conditions on the sphere surface, Equations 6 and 7, remain the same. However, the boundary conditions on the vapor–liquid interface may be specified, for the simplest cases at $y=\Delta$, as

$$u_v=0 \tag{42}$$

or

$$\frac{\partial u_v}{\partial y}=0 \tag{43}$$

and

$$T_v=T_{\text{sat}} \tag{44}$$

Equation 43 may be interpreted as a zero shear condition or a constant velocity condition. The solution to the set results in a linear temperature profile and two possibilities of a quadratic

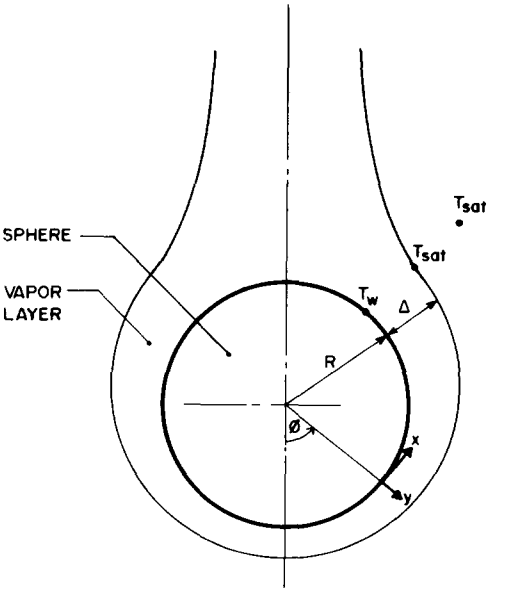

Figure 2 Model for saturated film boiling

velocity profile. The solution is identical to two of the four cases mentioned in Farahat and Nasr.[6] There, two additional cases are based on the assumption of a quadratic temperature profile, specified in the present formulation by the alternative boundary condition that, at $y=\Delta$,

$$\frac{\partial T_v}{\partial y}=0 \tag{45}$$

The profiles for the four cases are given in the Appendix.

From the heat balance relation (modified Equation 17), we can now solve for the vapor thickness:

$$\Delta=\left[\frac{c\mu_v k_v \Delta T_{sat} R}{g(\rho_l-\rho_v)h^*_{fg}\rho_v}\right]^{1/4} I(\phi) \tag{46}$$

where c takes on values of 16, 32, 4, and 8 for cases (a), (b), (c), and (d), respectively, as defined in the Appendix; $I(\phi)$ is as defined in Equation 23.

The average heat flux and average Nusselt number may now be obtained by the same procedure as in Equations 30 and 31. Using Equation 46, we get the final form:

$$\overline{Nu}_D=C'_o(Gr_D Pr^*_v)^{1/4} \tag{47}$$

where

$$Pr^*_v=\frac{(Pr_v)(2h^*_{fg})}{c_{p_v}\Delta T_{sat}} \tag{48}$$

and where C'_o takes on values 0.492, 0.828, 0.696, and 1.170, respectively, for the four cases. These values of C'_o are different from those reported in Farahat and Nasr,[6] as the method of averaging the Nusselt number is different there.

Comparison with experimental data

Comparison of theoretical results with experimental data is shown in Figures 3 and 4, where for clarity the range of experimental results for each set of film boiling is represented by a line connecting two identical symbols. As the usual quenching method is used for obtaining the boiling curves, the upper (right-hand side) symbol represents the start of film boiling, and the lower symbol represents the minimum film boiling point.

Figure 3 shows the comparison of subcooled data with Equation 33. The water data[9] are obtained by quenching a 30-mm-diameter silver sphere in water at six temperatures over a subcooling range of 80 K. By virtue of the high thermal conductivity of silver, the sphere may be regarded as a lumped-heat-capacity system, with its uniform temperature measured by a thermocouple. The heat transfer coefficient and hence the Nusselt number so calculated from the temperature versus time-quenching curve is thus recognized as an average value for the sphere. Agreement with Equation 33 is good, especially with ΔT_{sub} greater than 20 K.

Two sets of data for Freon-12 were obtained in our laboratory by quenching copper spheres of diameters 20 mm and 25 mm, respectively, into Freon-12 at seven temperatures over a subcooling range of 70 K. These data generally lie farther from the Equation 33 line than do the water data. For both the water and Freon-12 data, estimation of radiative losses indicates that they are negligible, and hence no correction is made on the raw data. Also shown in Figure 3 are the Freon-11 data from Shih and El-Wakil,[11] where subcooled boiling was carried out for a 3.175-mm brass sphere at five temperatures over a subcooling range of 20 K. They scatter above the theoretical line as much as the Freon-12 data.

Interestingly, the theoretical line forms the lower limit to all the data, suggesting that the model gives a conservative estimate of the film boiling heat loss. The upper bound of the data is at a C_o value of about 1.6, as indicated by the dashed line in Figure 3, compared to about 0.7 in Equation 41.

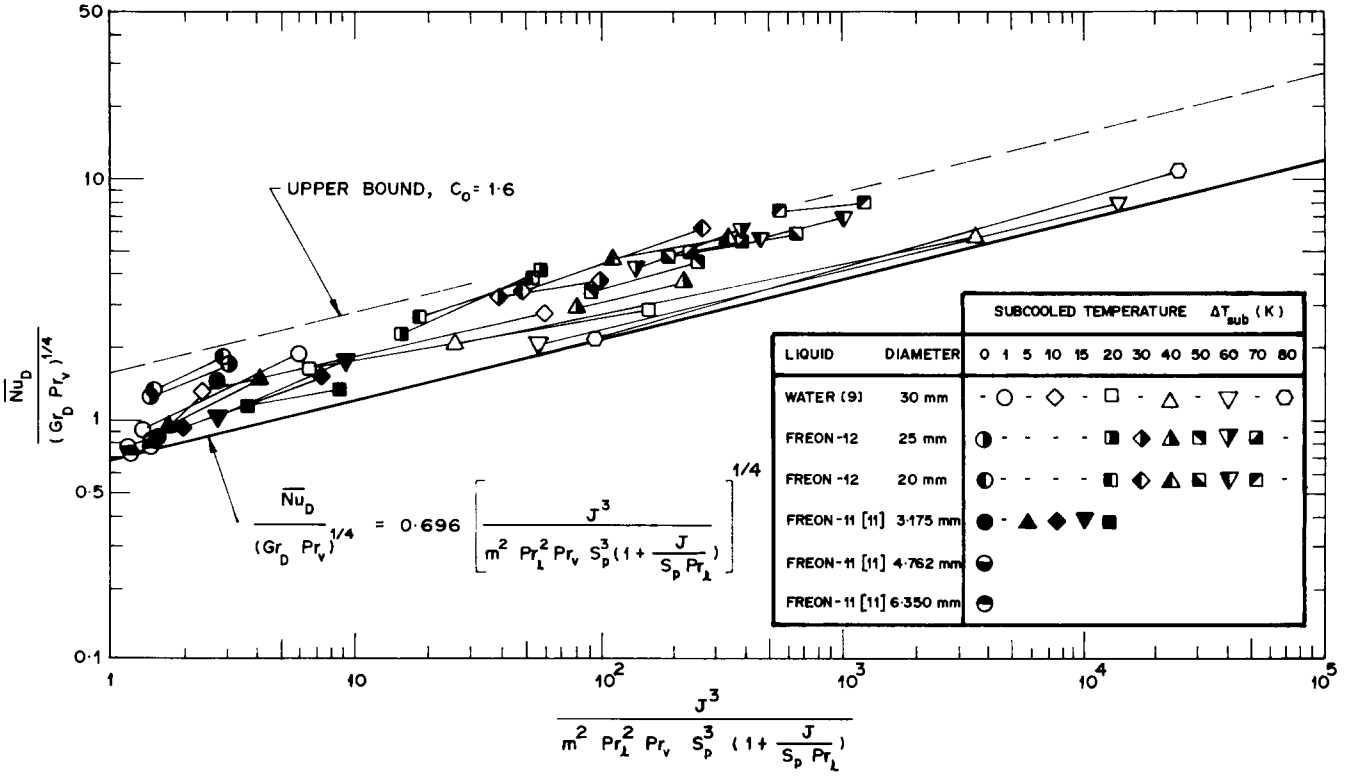

Figure 3 Comparison of subcooled data with Equation 33

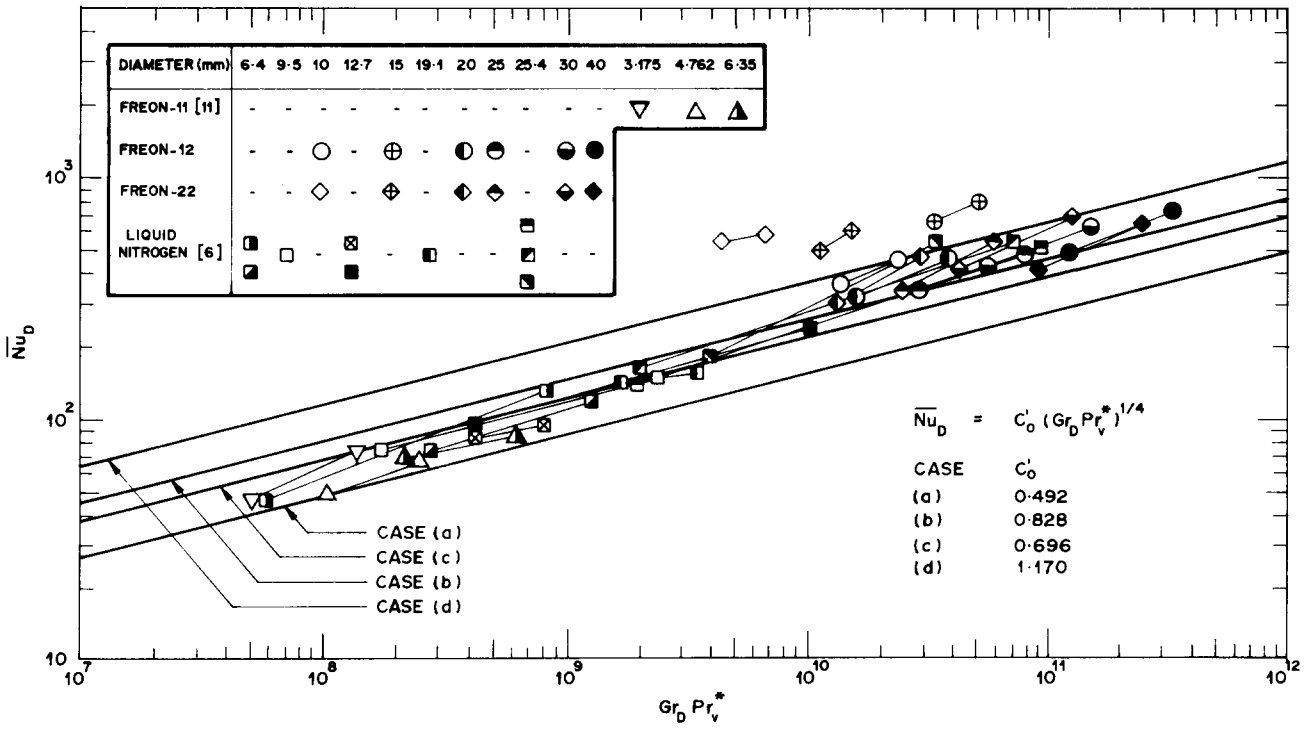

Figure 4 Comparison of saturated data with Equation 47

Turning now to Figure 4, we obtained experimental data for saturated boiling in Freon-12 and Freon-22 in our laboratory for six copper spheres with diameters ranging from 10 mm to 40 mm. Compared to the four lines representing the four cases of analysis, all the data lie between cases (b) and (d), except for the three sets that fall above the case (d) line. Other published data in Figure 4 are data from Shih and El-Wakil[11] for smaller spheres quenched in Freon-11, as well as a collection of data from Farahat and Nasr,[6] which are based on a survey of investigators[12–17] using liquid nitrogen as the boiling fluid. Most of the data lie within the zone defined by the lines for cases (a)–(d), with a gradual shift from case (a) to case (d) as the heat transfer coefficient increases. This shift seems to support a power of $\frac{1}{3}$ instead of $\frac{1}{4}$ for $(Gr_D Pr_v^*)$, as was concluded empirically[6] for the nitrogen data alone.

With respect to theory, accomplishing an analytical solution required many simplifying assumptions. We do not imply that the neglected effects, as well as other effects such as turbulence, properties of the boiling surface, surface tension, system pressure, or the vapor plume are unimportant in pool film boiling (e.g., see references 9, 10, and 16). Nevertheless, the analytical solutions do give some understanding of the roles played by the participating parameters in subcooled film boiling. The results seem encouraging enough to warrant further investigations of modeling to consider inclusion of other effects.

Conclusions

Further refinement of the analytical derivations for pool film boiling based on stated simplifications has been presented. From comparison with experiments, Equation 33 seems to bracket selected data well for subcooled boiling, with the coefficient C_o taking the range from the theoretically derived value of about 0.7 to an empirical upper limit of 1.6. For saturated boiling, the four cases of Equation 47 cover most of the data, although further investigation is warranted because none of the four cases satisfies the data completely.

Acknowledgment

This work is a result of JSPS-VCC cooperative research between Kyoto University and the University of Malaya. The authors gratefully acknowledge the suggestions and criticisms by Professor Itaru Michiyoshi and the assistance of his research group at Kyoto University.

References

1 Bromley, L. A. Heat transfer in stable film boiling. *Chem. Eng. Prog.*, 1950, **46**, 221–227
2 Koh, J. C. Y. Analysis of film boiling on vertical surfaces. *J. Heat Transfer*, 1962, **84**(1), 55–62
3 Sparrow, E. M. and Cess, R. D. The effect of subcooled liquid on laminar film boiling. *J. Heat Transfer*, 1962, **84**(2), 149–156
4 Nishikawa, K. and Ito, T. Two-phase boundary layer treatment of free-convection film boiling. *Int. J. Heat Mass Transfer*, 1966, **9**, 103–115
5 Frederking, T. H. K. and Clark, J. A. Natural convection film boiling on a sphere. *Adv. Cyrog. Eng.*, 1962, **8**, 501–506

6 Farahat, M. M. and Nasr, T. N. Natural convection film boiling from spheres to saturated liquids, an integral approach. *Int. J. Heat Mass Transfer*, 1978, **21**, 256–258

7 Nakayama, A. and Koyama, H. An integral method in laminar film pool boiling from curved surfaces. *J. Heat Transfer*, 1986, **108**, 490–493

8 Nishikawa, K., Ito, T., Matsumoto, K., and Kuroki, T. A correlation of pool film boiling heat transfer from a horizontal cylinder of uniform surface temperature to subcooled liquids. *Technology Reports of Kyushu University*, 1975, **48**(6), 815–821 (in Japanese)

9 Michiyoshi, I., Takahashi, O., and Kikuchi, Y. Heat transfer and the low limit of film boiling. *Proc. of the First World Conference on Experimental Heat Transfer, Fluid Mechanics and Thermodynamics*, Dubrovnik, Yugoslavia, Sept. 4–9, 1988, 1404–1415

10 Westwater, J. W., Hwalek, J. J., and Irving, M. E. Suggested standard method for obtaining boiling curves by quenching. *I&EC Fundamentals*, 1986, **25**(4), 685–692

11 Shih, C. and El-Wakil, M. M. Film boiling and vapor explosions from small spheres. *Nuc. Sci. Eng.*, 1981, **77**, 470–479

12 Frederking, T. H. K., Chapman, R. C., and Wang, S. Heat transfer and fluid motion during cooldown of single bodies to low temperatures. *Adv. Cyrog. Eng.*, 1965, **10**, 353–360

13 Merte, J. E. and Clark, J. A. Boiling heat transfer with cryogenic fluids at standard, fractional, and near zero gravity. *J. Heat Transfer*, 1964, **86**, 351–359

14 Daniels, D. J. Film-boiling two-phase flow. M.S. thesis, University of California at Los Angeles, 1965

15 Rhea, L. G. and Nevins, R. G. Film boiling heat transfer from an oscillating sphere. *J. Heat Transfer*, 1969, **91**, 267–272

16 Hendricks, R. C. and Baumeister, K. J. Film boiling from submerged spheres. NASA TND-5124, Lewis Research Center, Cleveland, USA, 1969

17 Rhea, L. G. Boiling heat transfer from an oscillating sphere with a cryogenic fluid at atmospheric pressure and standard gravity. Ph.D. dissertation, Kansas State University, 1967

Appendix

Profiles for the four cases in saturated boiling

- Case (a)—*Boundary Conditions (Equations 6, 7, 42, and 44):*

$$u_v=\frac{\Delta^2 g(\rho_l-\rho_v)\sin\phi}{2\mu_v}\left[\frac{y}{\Delta}-\left(\frac{y}{\Delta}\right)^2\right] \tag{A.1}$$

$$T_v=T_w-\frac{\Delta T_{\text{sat}}\, y}{\Delta} \tag{A.2}$$

- Case (b)—*Boundary Conditions (Equations 6, 7, 43, and 44):*

$$u_v=\frac{\Delta^2 g(\rho_l-\rho_v)\sin\phi}{2\mu_v}\left[2\left(\frac{y}{\Delta}\right)-\left(\frac{y}{\Delta}\right)^2\right] \tag{A.3}$$

$$T_v=T_w-\frac{\Delta T_{\text{sat}}\, y}{\Delta} \tag{A.4}$$

- Case (c)—*Boundary Conditions (Equations 6, 7, 42, and 45):*

$$u_v=\frac{\Delta^2 g(\rho_l-\rho_v)\sin\phi}{2\mu_v}\left[\frac{y}{\Delta}-\left(\frac{y}{\Delta}\right)^2\right] \tag{A.5}$$

$$T_v=\Delta T_{\text{sat}}\left(1-\frac{y}{\Delta}\right)^2+T_{\text{sat}} \tag{A.6}$$

- Case (d)—*Boundary Conditions (Equations 6, 7, 43, and 45):*

$$u_v=\frac{\Delta^2 g(\rho_l-\rho_v)\sin\phi}{2\mu_v}\left[2\left(\frac{y}{\Delta}\right)-\left(\frac{y}{\Delta}\right)^2\right] \tag{A.7}$$

$$T_v=\Delta T_{\text{sat}}\left(1-\frac{y}{\Delta}\right)^2+T_{\text{sat}} \tag{A.8}$$